Journal of Zoological Systematics and Evolutionary Research

WILEY

RESEARCH ARTICLE OPEN ACCESS

Drawing the Vine Line: Integrative Analyses Reveal Seven Distinct Species of African Vine Snakes, *Thelotornis* (Colubridae: Colubrinae)

Hanlie M. Engelbrecht[1] | Kutloano L. Seeiso[1] | Thomas G. Eimermacher[2] | Harith Farooq[3] | Michele Menegon[4,5] | Werner A. Conradie[6,7]

[1]School of Animal, Plant and Environmental Sciences, University of the Witwatersrand, Johannesburg, South Africa | [2]Collin College, McKinney, Texas, USA | [3]Faculty of Natural Sciences, Lúrio University, Pemba, Mozambique | [4]MUSE, Museo delle Scienze, Viale del Lavoro e delle Scienza, 3, Trento 38122, Italy | [5]PAMS Foundation, Arusha, Tanzania | [6]Port Elizabeth Museum (Bayworld), P.O. Box 13147, Humewood 6013, South Africa | [7]Department of Nature Conservation Management, Natural Resource Science and Management Cluster, Faculty of Science, Nelson Mandela University, George Campus, George, South Africa

Correspondence: Hanlie M. Engelbrecht (hanlie.engelbrecht@wits.ac.za)

Received: 28 November 2025 | **Revised:** 28 December 2025 | **Accepted:** 14 January 2026

Academic Editor: Fabricius Domingos

Keywords: Africa | cryptic species | reptiles | serpentes | squamata

ABSTRACT

African Vine Snakes of the genus *Thelotornis* are highly specialised arboreal colubrids distributed across sub-Saharan Africa. Despite pronounced morphological conservatism, the genus occupies diverse forest, woodland and savanna-associated habitats. The genus has long been characterised by unresolved species boundaries and taxonomic uncertainty, particularly regarding the placement of the monotypic *Xyelodontophis uluguruensis*. We investigated phylogenetic relationships and species boundaries within *Thelotornis* using an integrative framework with broad geographic and ecological sampling. Phylogenetic inference was based on two mitochondrial (cyt b and ND4) and two nuclear (c-mos and NT3) markers analysed under maximum-likelihood (IQ-TREE2) and multispecies coalescent (Species Tree And Classification Estimation, Yarely [STACEY]) frameworks. Species boundaries were further assessed using haplotype networks, mitochondrial divergence, single-locus barcoding (Assemble Species by Automatic Partitioning [ASAP]) and unsupervised machine learning (UML) clustering (super self-organising map [SuperSOM]) integrating genetic, morphological, ecological and spatial data. Seven independently evolving lineages are supported, with *Thelotornis* monophyletic only when *Xyelodontophis uluguruensis* is included. *Thelotornis capensis* subspecies are recognised as distinct species, and an undescribed lineage from Vamizi Island, Mozambique, has been identified. Emergence of the genus trace to the Mid-Miocene (*ca*. 16.6 Mya), with Late-Miocene diversification giving rise to a West–East African forest lineage (*T. kirtlandii* and *T. uluguruensis* comb. nov.) and an East–Southern African lineage comprising habitat generalists (*T. usambaricus*, *T.* sp., *T. mossambicanus* and *T. capensis*) alongside the savanna specialist *T. oatesi* stat. nov. Morphological, ecological and genetic evidence support the distinctiveness of all seven lineages, informing a revised diagnosis of *Thelotornis*. These results indicate a recent ecological radiation shaped by historical habitat dynamics, facilitating forest niche conservatism while ecological opportunity enabled savanna diversification, resolving taxonomic ambiguity and revealing hidden diversity.

1 | Introduction

Vine snakes are characterised by a suite of morphological and behavioural specialisations associated with an arboreal habitus and, in many respects, represent the extreme of such adaptations [1–3]. They are among the most specialised lineages for navigating structurally complex forest and savanna habitats, characterised by markedly elongated, slender bodies and tails, cryptic colouration and large and horizontally or keyhole-shaped pupils that enhance camouflage and visual acuity. Despite these striking phenotypic similarities, vine snakes comprise at least three geographically disparate and phylogenetically distant colubrid genera: the Asian genus *Ahaetulla* (Ahaetuliinae), the American *Oxybelis* (Colubrinae) and the African *Thelotornis* (Colubrinae) [4, 5]. Among these, *Thelotornis* provides a particularly compelling system for examining how African historical landscape dynamics may have shaped lineage diversification under strong ecological constraints.

Thelotornis belongs to an African arboreal colubrid radiation that comprises two tribes, Philothamni and Dispholidini [6]. The genus is placed within the Dispholidini, a clade that includes two major groups distinguished by maxillary dentition and venomous state. The opisthoglyphous, haemotoxic genera include *Dispholidus* and *Thelotornis*, whereas the aglyphous genera comprise *Thrasops*, *Rhamnophis*, and the monotypic *Xyelodontophis uluguruensis*. Under current taxonomy, *Thelotornis* include four species and one subspecies: *T. usambaricus*, *T. kirtlandii*, *T. mossambicanus*, *T. capensis capensis* and *T. c. oatesi* [7, 8]. Collectively, these taxa are distributed across tropical and subtropical regions of sub-Saharan Africa, including an insular population on Vamizi Island, off the northern coast of Mozambique [9–12].

The broad geographic distribution and ecological similarity among the African Vine Snakes obscure the extent to which external morphology corresponds to independently evolving lineages, highlighting the need for phylogenetic and integrative analyses of species boundaries. Historically, in the absence of phylogenetic data, species and subspecies were defined using traditional characters such as lepidosis, colouration, particularly of the head and neck (Figure 1), hemipenile morphology and visceral anatomy [8, 13]. However, cryptic species resulting from morphological conservatism are increasingly recognised among arboreal colubrids, including members of the Dispholidini and Philothamni tribes, suggesting that nominal species boundaries within *Thelotornis* may not fully capture evolutionary history ([14–16]; Madsen et al. in prep.). For example, *Xyelodontophis* is morphologically very similar to *Thelotornis*, differing primarily in dentition, with three dagger-shaped aglyphous posterior maxillary teeth, and in having a pear-shaped rather than keyhole-shaped pupil [13]. Furthermore, unpublished work indicates that *Xyelodontophis* is phylogenetically nested within *Thelotornis* [17], raising questions about the monophyly of *Thelotornis* and the validity of the monotypic generic status of *Xyelodontophis*.

These unresolved taxonomic patterns are best interpreted within the broader evolutionary and biogeographic history of sub-Saharan Africa. *Thelotornis* has a Mid-Miocene stem age of approximately 16–17 Mya [18] and occurs across ecologically

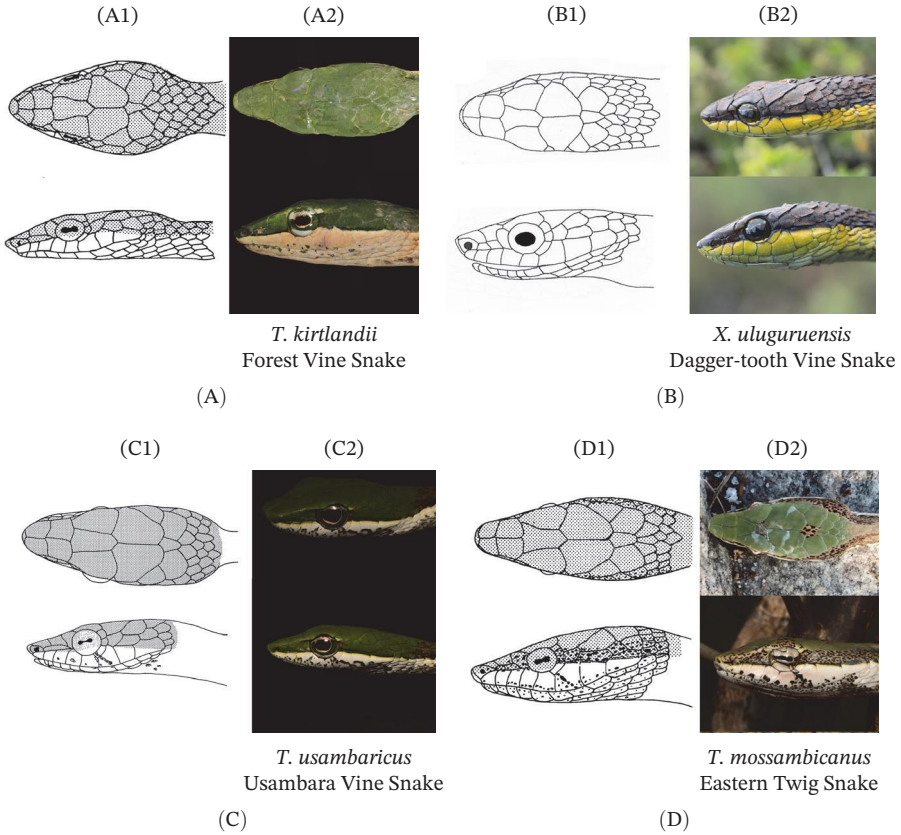

FIGURE 1 | (Continued)

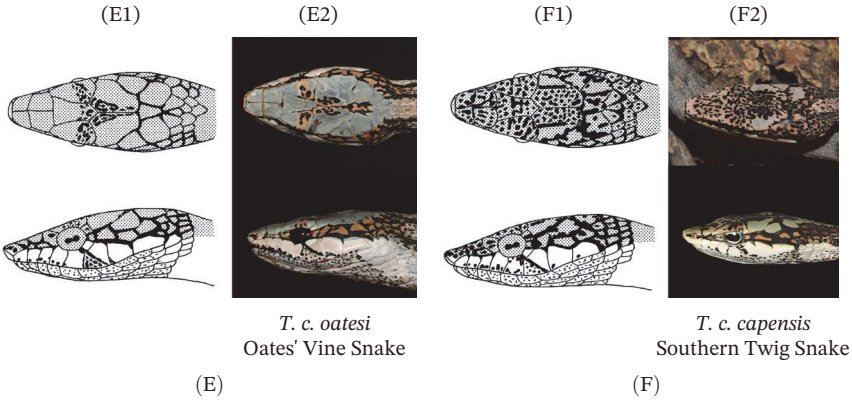

FIGURE 1 | *Thelotornis* variation in head scale pattern and colouration. (A1, B1, C1, D1, E1, F1) Line drawings highlighting dorsal and lateral head scales (adapted from Broadley [8] and Broadley and Wallach [13]), (A2, B2, C2, D2, E2, F2) corresponding colour photographs of the same species. Six species recognised based on existing species diagnoses using scale and colour patterns: (A) *T. kirtlandii* [Mt Tokedah, Liberia], (B) *X. uluguruensis* [Mkingu Nature Forest Reserve, Nguru Mountains, Tanzania], (C) *T. usambaricus* Mkingu Nature Forest Reserve, Nguru Mountains, Tanzania, (D) *T. mossambicanus* [Top: Pemba, Mozambique (https://www.inaturalist.org/observations/273566082); Bottom: Ribuae, Mozambique]; (E) *T. capensis oatesi* [Longa, Angola] and (F) *T. c. capensis* [Top: Polokwane, South Africa; Bottom: Tshaulu, South Africa]. Photo credits: A – William R. Branch; B, C – Michele Menegon; D – Florencio Thompson (Top), Werner Conradie (bottom); E – Werner Conradie; F – Ruan Stander. One additional undescribed species from Vamizi Island, Mozambique, is not included here.

and geologically dynamic regions that have experienced recurrent forest contraction, climatic oscillations, tectonic activity and a gradual shift toward savanna dominance since the Miocene [19–23]. Given the arboreal habitus of African Vine Snakes, historically stable refugial areas such as coastal and montane forests may have preserved isolated forest-specialist lineages. At the same time, Miocene heterogeneous forest and savanna mosaics may have facilitated the emergence of forest–savanna generalists, which could have tracked transitional habitats via arid corridors, potentially leading to allopatric, parapatric or ecologically structured divergence. Conserved morphological variation, however, may obscure these historical patterns, resulting in cryptic diversity despite limited phenotypic differentiation (e.g., [7, 8, 13–15]). Placing *Thelotornis* within a historical biogeographic framework, therefore, provides a powerful means of interpreting speciation processes and identifying evolutionarily independent lineages by linking geographic, ecological and climatic dynamics to lineage divergence. This interpretation aligns with broader patterns documented in African vertebrates with comparable distributions and emergence times (e.g., [24–26]), highlighting the value of biogeography as a mechanistic basis for delimiting species boundaries in arboreal forest-associated snakes [27].

We anticipated that lineage diversification within *Thelotornis* primarily occurred during the Mid-Miocene to Late-Miocene, coinciding with pronounced forest fragmentation and the rapid expansion and stabilisation of savanna biomes driven by tectonic uplift, climatic oscillations and long-term aridification in Africa. Given the potential for conserved morphological variation to mask cryptic diversity, we evaluated the monophyly of African vine snakes (*Thelotornis* spp.) relative to the monotypic Dagger-tooth Vine Snake (*Xyelodontophis uluguruensis*) and assessed morphological species under the Unified Species Concept (USC) [28, 29]. The USC defines species as independently evolving lineages and integrates multiple operational criteria for delimitation. Phylogenetic relationships and species boundaries were examined using barcoding-based species delimitation, a multi-species coalescent probabilistic model and an integrative framework combining molecular data, morphological characters, macro- and micro-habitat associations and spatial information. We also estimated patterns of intra-generic lineage diversification. By integrating these complementary lines of evidence, we were able to rigorously test whether currently recognised *Thelotornis* lineages meet species-level criteria under the USC. We refine African Vine Snake taxonomy accordingly, while advancing conceptual understanding of how historical landscape changes, ecological specialisation and cryptic diversity interact to drive speciation in Africa's arboreal fauna.

2 | Materials and Methods

2.1 | Taxon Sampling

Ingroup taxa included in the study were *Thelotornis c. capensis* ($n = 11$), *T. c. oatesi* ($n = 8$), *T. kirtlandii* ($n = 10$), *T. mossambicanus* ($n = 9$), *Thelotornis* sp. from Vamizi Island—off the northern coast of Mozambique (previously assigned to *T. usambaricus*; fide [9]; $n = 3$), *T. usambaricus* ($n = 6$) and *Xyelodontophis uluguruensis* ($n = 3$). Tissue samples and sequence data were sourced from the South African National Biodiversity Institute BioBank, from specimens collected during fieldwork by Harith Farooq, Hanlie Engelbrecht M., Michele Menegon, Thomas G. Eimermacher, Werner Conradie and from GenBank (Supporting Information 1). Geographical sampling per taxon broadly represents species' distribution based on Broadley [8].

2.2 | DNA Extraction, Amplification and Sequencing

To investigate the phylogenetic relationships among the focal species, genomic DNA was used to amplify and sequence a combination of two slow-evolving nuclear protein-coding markers—neurotrophin-3 (NT3; primers: NT3-F3 and NT3-R4 [30]) and oocyte maturation factor c-mos (c-mos; primers: S77 and S78, [31])—as well as two mitochondrial protein-coding genes: cytochrome *b* (cyt *b*; primers: L14910 and H16064 [32, 33]) and

NADH dehydrogenase subunit 4 (ND4; primers: NADH4 and HIS12763V [34, 35]). Genomic DNA was extracted from tissue samples using commercial DNA extraction kits (E.Z.N.A. Tissue DNA Kit, Omega Bio-tek and QIAgen Blood and Tissue kit (QIAgen Inc., Canada)), following the manufacturer's protocol, as well as a salt extraction protocol [36]. The quality of extracted genomic material was verified using a Thermo Scientific NanoDrop One^C Microvolume UV–Vis Spectrophotometer. Amplification of the relevant gene regions was done using 25 μL reaction volumes that contained: genomic DNA, dH_2O, 10x thermophilic buffer, 2.5 mM $MgCl_2$, forward and reverse primers of each relevant marker, 0.2 mM dNTPs and 0.2 U Super-Therm Taq DNA polymerase. The polymerase chain reaction (PCR) had a denaturation step of 4 min at 94°C, then 32 cycles of denaturation (40 s at 94°C), annealing (40 s at 48–64°C) and extension (1 min at 72°C) and was ended with a final extension step of 10 min 72°C.

2.3 | Phylogenetic and Multi-Species Coalescent Inference

Sequences for each DNA marker were aligned separately using MEGA 11 [37]. Alignments were checked for ambiguities, manually refined where necessary, trimmed and inspected for stop codons. Final alignment lengths were 572 bp for c-mos, 506 bp for NT3, 605 bp for cyt *b* and 621 bp for ND4. All protein-coding genes (c-mos, NT3, cyt *b* and ND4) were analysed both under codon-partitioned models and by grouping codon Positions 1 and 2 versus Position 3. To account for differences in mutation rates among the four markers and to maximise phylogenetic resolution across timescales, we analysed two complementary datasets: Dataset 1 combining all four markers (c-mos + NT3 + cyt *b* + ND4), and Dataset 2 comprising only mitochondrial regions (cyt *b* and ND4), which are particularly informative for recent divergences and species boundary inference [38].

To reconstruct phylogenetic relationships within *Thelotornis* and evaluate the placement of *Xyelodontophis uluguruensis* relative to *Thelotornis*, we included out-group taxa representing additional members of Dispholidini (*Dispholidus typus*, *Rhamnophis batesii* and *Thrasops jacksonii*), representatives of the sister tribe Philothamnini (*Hapsidophrys smaragdina* and *Philothamnus hoplogaster*) and the more distantly related colubrid *Ptyas mucosa*. Maximum likelihood phylogenetic trees were constructed using the ultrafast bootstrap method with 1000 replicates and the best-fit DNA substitution model identified via ModelFinder under site-specific partitioning, as implemented in IQ-TREE2 [39–44]. Branch support was also evaluated using the SH-like approximate likelihood ratio test (SH-aLRT), with 1000 replicates. Likelihood scores were compared across topologies to identify the best-supported phylogenetic hypothesis. Species relationships were considered strongly supported when node values met the thresholds of UFBoot2 ≥95% and SH-aLRT ≥80% [42, 43, 45].

We further estimated a species tree for *Thelotornis* under the multi-species coalescent framework implemented using the Species Tree And Classification Estimation, Yarely (STACEY) package in Bayesian evolutionary analysis by sampling trees [46–48]. STACEY jointly infers lineage diversification, species delimitation and species tree topologies by modelling gene tree discordance under the multi-species coalescent with a birth–death-collapse prior on lineages. The dataset comprised sequences from two mitochondrial genes (ND4 and cyt *b*) and one nuclear gene (c-mos), selected to maximise taxon coverage across in-group and out-group taxa and to enable the placement of reliable calibration points. Each marker was treated as a separate partition. Heterozygous sites in the nuclear marker were retained, and phasing was integrated over by STACEY during the analysis, removing the need for prior allele phasing. Substitution, clock and site models were unlinked across loci, and an uncorrelated log-normal relaxed clock was applied to each [49]. Taxon sets were fixed a priori, considering all currently recognised species and subspecies and the insular population; *T.* sp. as distinct taxa.

2.4 | Multi-Species Coalescent Lineage Diversification

To estimate divergence times via STACEY, we applied fossil- and biogeography-informed calibration points as log-normal priors. The first calibration was placed on the divergence between eastern and western *Hemorrhois* lineages (*H. ravergieri* + *H. nummifer* vs. *H. algirus* + *H. hippocrepis*), informed by evidence that divergence followed the collision of the Africa–Arabia plate with Eurasia approximately 16–18 Mya [50]. The second calibration constrained the most recent common ancestor of *Dolichophis*, *Hierophis* and *Eirenis*, based on fossil evidence for a minimum age of 18 Mya [51]. Both calibrations were implemented in real space as log-normal priors with means of 17.0 and 18.0, $\sigma = 0.5$ and offsets of 0.0 (Supporting Information 2). Six independent MCMC runs were performed, each for 1,000,000,000 states, sampling every 10,000 states, implemented in the BEAST2 XSEDE on CIPRES Science Gateway (www.phylo.org). Log and tree files from individual runs were combined using LogCombiner v2.7.8 (part of BEAST 2.7.8; [46, 52]), applying a 10% burn-in to the log files. Convergence and mixing were assessed in Tracer v1.7 [53], with effective sample sizes (ESSs) >200 considered indicative of sufficient sampling [54]. Posterior trees from combined runs were summarised in TreeAnnotator (part of BEAST 2.7.8; [46, 52]) to produce a maximum clade credibility (MCC) tree using median node heights, which was visualised and annotated in FigTree v1.4.4 [53].

2.5 | Species Delimitation

To investigate species boundaries within *Thelotornis*, we employed an integrative workflow combining genetic barcoding, sequence divergence analyses, haplotype networks and Bayesian species delimitation using STACEY with STACEY Species Delimitation Analyzer (SDA), alongside an integrative approach incorporating DNA, morphology, spatial and habitat data.

Genetic barcoding enables rapid, objective partitioning of sequences with minimal subjective bias. We applied Assemble Species by Automatic Partitioning (ASAP) [55] to mtDNA loci, identifying putative species boundaries by analysing genetic distances to detect barcode gaps and partition sequences accordingly. Species by automatic partitioning evaluates alternative partitions using a scoring system based on intra-group divergence, barcode-gap width and an approximation of panmixia, assigning each partition an ASAP score that reflects its relative support. Analyses were performed via

the ASAP web-interface (https://bioinfo.mnhn.fr/abi/public/asap) using mtDNA loci with default settings.

To complement the barcoding analyses, we calculated uncorrected pairwise and average sequence divergence for cyt *b* and ND4 between individuals and lineages in MEGA 12 [56]. To explore intraspecific variation and assess lineage coherence, we constructed mitochondrial haplotype networks for cyt *b*. Unique haplotypes were identified using DnaSP v6, and networks were visualised in PopArt v1.7 under a statistical parsimony framework [57, 58]. These networks were examined to assess concordance with species boundaries inferred from ASAP and to detect substructure within lineages, providing an additional perspective on species-level differentiation.

To evaluate species boundaries using the STACEY outputs, we implemented the STACEY SDA [47] in R Studio, using the following packages: ape [59] and phangorn [60] for phylogenetic tree manipulation, dplyr [61] and tidyr [62] for data wrangling, stringr [63] for string operations and ggplot2 [64] and readr [65] for visualisation and data import. The analysis used the same molecular dataset and partitions as the divergence dating analysis, with taxon sets defined a priori for all currently recognised species and subspecies, including *T*. sp. The STACEY SDA estimates the probability that each lineage represents an independently evolving unit by integrating over gene tree discordance under the multi-species coalescent. Lineage stability was quantified as the proportion of the posterior distribution in which each focal lineage was consistently recovered within the same cluster, providing a probabilistic framework for assessing species-level distinctiveness. The analysis was configured with a collapse height of 1.0E-4 and a collapse weight of 0.5, that is, conservative settings favouring lumping of lineages unless strongly supported by the data.

The integrative, unsupervised machine learning (UML) super self-organising maps (SuperSOMs; [66]) approach was used to project high-dimensional input data into a low-dimensional space to estimate species clustering. The input data consisted of a multi-layered matrix linking individual specimens to multiple data types, including molecular data, traditional morphological characters following Broadley [8] and Broadley and Wallach [13], spatial coordinates and ecological attributes such as macrobiome and microhabitat affiliation based on the Terrestrial Ecoregions of the World [67]. For the molecular data layer, individual-level aligned DNA sequence data were encoded by converting each nucleotide state at every alignment position into a numeric variable, thereby transforming the multiple sequence alignment into a high-dimensional genetic feature matrix suitable for SOM–based clustering. Distance weights were calculated for each data layer and normalised to the interval 0–1 to ensure equal contributions to clustering while providing empirical estimates of relative importance.

Cluster number (K) was determined using K-means clustering of SuperSOM grid cells, evaluating the total weighted sum of squares (WSS) across $K = 2$–10. The number of biologically meaningful clusters was taken where within-cluster variance plateaued and cluster assignments converged across data layers. We also explicitly tested multiple delimitation hypotheses reflecting current taxonomy and putative species boundaries: (1) $K = 4$, grouping taxa by traditional morphology (*X. uluguruensis*, *T. kirtlandii*, *T. usambaricus* (including *T*. sp. from Vamizi Island) and *T. capensis sensu lato*, here considered as *T. c. capensis*, *T. c. oatesi*, and *T. mossambicanus* fide Broadley [7]); (2) $K = 5$, treating *T. mossambicanus* as a full species fide Broadley [8]; (3) $K = 6$, treating the two *T. capensis* subspecies as full species; (4) $K = 7$, treating all focal lineages and subspecies as distinct species (*X. uluguruensis*, *T. kirtlandii*, *T. usambaricus*, *T*. sp., *T. mossambicanus*, *T. c. capensis* and *T. c. oatesi*). The UML SuperSOM integrative species delimitation analysis was implemented in R Studio (version 2022.12.0 + 353;[68]) using R (version 4.2.2;[68]) and the following packages: APE v5.0 for loading genetic data [69], kohonen v3.0.12 for training and constructing SOMs [70], factoextra v1.0.7 for visualising optimal cluster numbers [71], cluster v2.1.6 for clustering analyses [72], Rtsne v0.17 for converting high-dimensional genetic data to low-dimensional numeric matrices [73–75] and NbClust v3.0.1 for determining the optimal number of clusters in the dataset [76].

3 | Results

3.1 | Phylogenetic and Multi-Species Coalescent Inference

Maximum likelihood tree topologies, associated likelihood scores and selected DNA substitution models were comparable between data partitions tested for each marker separately, regardless of whether branch lengths were linked or allowed to vary independently across partitions. For most codon Positions 1 and 2 of protein-coding markers, simpler models with fewer assumptions and free parameters were selected. In contrast, codon Position 3 of protein-coding markers was best fit by more complex models, which incorporate additional parameters to account for the observed patterns in the sequence data. Log-likelihood values for phylogenetic trees—that is, gene trees and the two primary data compositions constructed in our study—are not directly comparable across analyses, as datasets differ in DNA marker composition, mutation rates and taxon coverage. Thus, a more negative log-likelihood does not necessarily indicate a worse tree; it may simply reflect a more complex dataset. Accordingly, we report phylogenetic patterns for our two primary DNA datasets: Dataset 1, c-mos + NT3 + cyt *b* + ND4 (log-likelihood = −15,694.606) and Dataset 2, mitochondrial loci cyt *b* + ND4 (log-likelihood = −7699.210). Seven well-supported monophyletic clades (SH-aLRT >80%, UFBoot >95%) were consistently recovered across both topologies (Figure 2A,B). These include *Xyelodontophis uluguruensis*, which is nested within *Thelotornis*, rendering the latter paraphyletic. The six remaining clades were: *Thelotornis kirtlandii*, *T. usambaricus*, *T*. sp., *T. mossambicanus*, *T. c. capensis* and *T. c. oatesi*.

The inclusion of *Xyelodontophis uluguruensis* within *Thelotornis* was well-supported across both ML analyses (Datasets 1 and 2), although its position relative to other *Thelotornis* species remains unresolved (Figure 2A,B and Supporting Information 3). The total-evidence dataset; Dataset 1 (Figure 2A), furthermore places *T*. sp. as sister to two partially supported clades (SH-aLRT >80%): *T. usambaricus* + *T. mossambicanus* and *T. c. capensis* + *T. c. oatesi*, with the sister relationship between *T. usambaricus* and T. *mossambicanus* supported only by SH-aLRT. An alternative hypothesis, based on the mtDNA topology, Dataset 2 (Figure 2B), suggests that *T. usambaricus* is sister to *T*. sp. + [*T. mossambicanus* + [*T. c.*

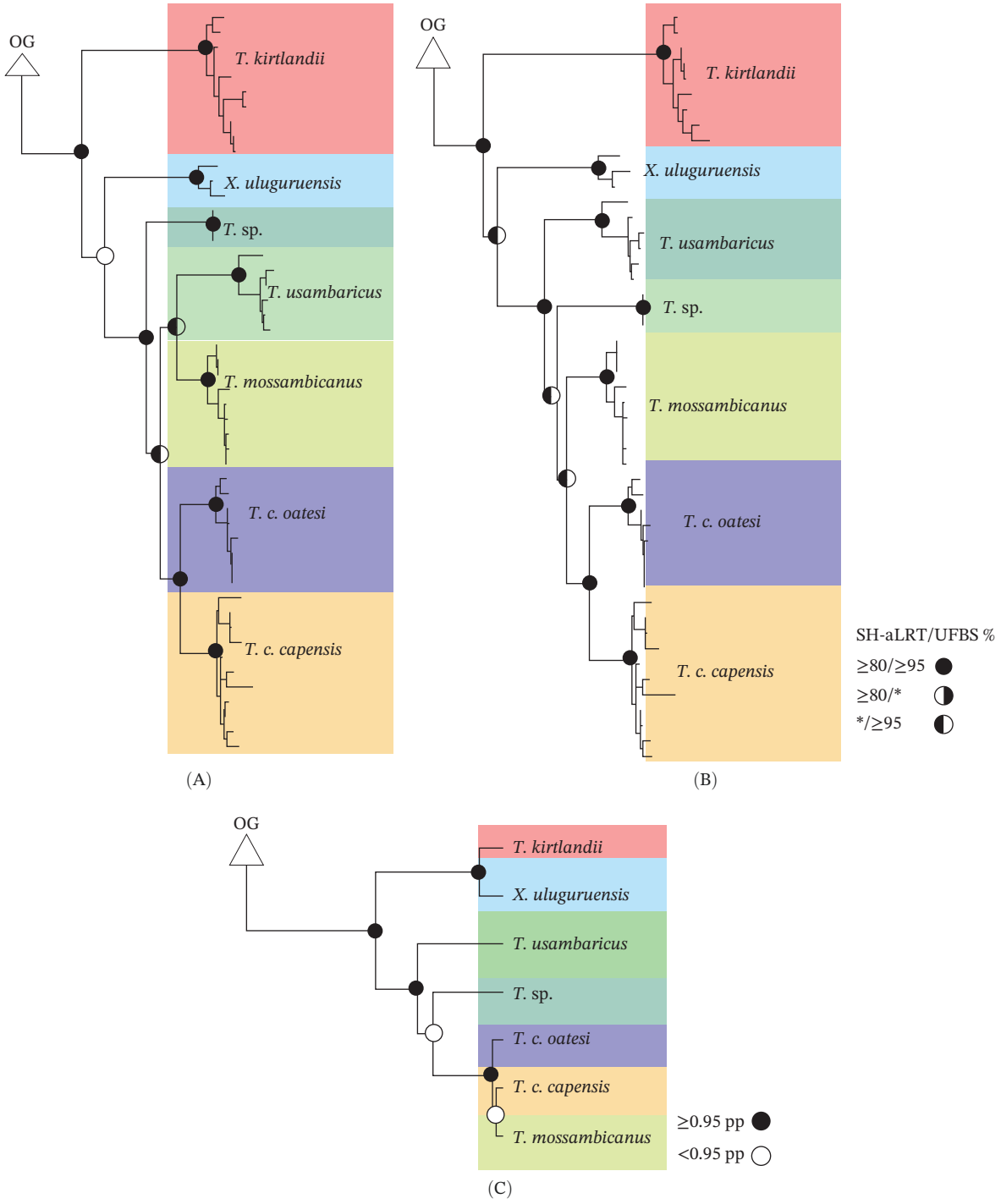

FIGURE 2 | Phylogenetic relationships of *Thelotornis* inferred from nuclear and mitochondrial markers and coalescent analysis. (A) Maximum-likelihood tree from total evidence including nuclear (c-mos, NT3) and mitochondrial genes (cyt *b* and ND4). (B) Maximum-likelihood tree from mitochondrial genes only (cyt *b* and ND4). (A, B) Node support is represented as SH-aLRT/UFBoot values, with supported nodes (SH-aLRT ≥80% and UFBoot ≥95%) indicated as black half circles. Branch lengths are scaled to the number of substitutions per site. (C) Coalescent species tree inferred with STACEY, showing posterior probabilities at nodes. Posterior probabilities ≥0.95 are considered supported and indicated as black circles at nodes.

capensis + *T. c. oatesi*]], and indicates that *T. c. capensis* and *T. c. oatesi* form two well-supported, distinct clades.

The multi-species coalescent tree indicates an overall well-resolved topology for *Thelotornis*, with high posterior support at most nodes (Figure 2C). *Xyelodontophis uluguruensis* was confirmed to be nested within the genus. Low posterior support is restricted to two nodes: the unresolved placement of *T.* sp. and the uncertain sister relationship between *T. capensis* and *T. oatesi*.

3.2 | Multi-Species Coalescent Lineage Diversification

Divergence time estimates were broadly consistent with previous studies (e.g., [18, 25]). The stem age of *Thelotornis* is estimated at approximately 16.61 Mya (Mid-Miocene), representing the split from its sister genus, *Dispholidus*. Intrageneric diversification commenced around 8.25 Mya, giving rise to two geographically and ecologically distinct lineages (Figure 3): a West–East African

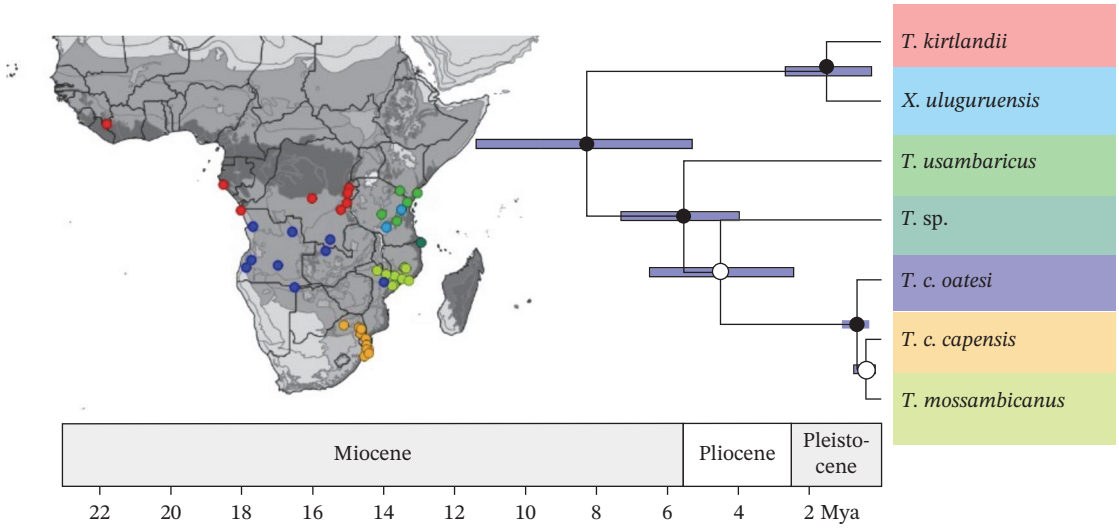

FIGURE 3 | Temporal and biogeographic context of *Thelotornis* diversification. The coalescent species tree (STACEY) shows median divergence dates for lineages, with node bars representing 95% highest posterior density intervals. Sampled localities for the dataset are shown on the accompanying biome map [67]. Shading intensity ranges from dark to light, corresponding to a continuum from closed forest habitats to open habitats (including savanna).

species assemblage (comprising *T. kirtlandii* and *X. uluguruensis*) confined to the Congolian forest belt and an East–Southern African species assemblage (*T. usambaricus*, *T.* sp., *T. mossambicanus*, *T. c. oatesi* and *T. c. capensis*), occupying forest-savanna mosaics and savanna. Subsequent divergence events occurred sequentially within the East–Southern lineage: *T. usambaricus* diverged at approximately 5.54 Mya, followed shortly by *T.* sp. at *ca*. 4.51 Mya. *Thelotornis c. oatesi* emerged *ca*. 0.67 Mya and the most recent divergence occurred at *ca*. 0.42 Mya, separating *T. c. capensis* and *T. mossambicanus*. These results are consistent with the hypothesis that *Thelotornis* lineage diversification commenced during the Mid–Late Miocene, coinciding with major forest fragmentation and habitat shifts in East Africa.

3.3 | Species Delimitation

Among the species delimitation scenarios generated by ASAP, the scheme with the lowest (i.e., best) ASAP score—ranked first in the analysis—identified seven putative species based on the mtDNA dataset. The seven putative species correspond to the seven major phylogenetic clades (Figures 2 and 4). The resulting ASAP barcoding gap was $d_T = 3.4\%$ for the mtDNA loci (cyt *b* + ND4) between ingroup taxa (Figure 4A). Complementary mean uncorrected pairwise sequence divergences for the cyt *b* dataset, between *Thelotornis* and *Xyelodontophis* lineages ranged from 4.91% to 12.37%. We interpret sequence divergence in the context of the phylogenetic relationships (Figure 2A), where clades with low divergence correspond to closely related lineages, and higher divergences align with more deeply divergent clades. Within *Thelotornis*, the lowest divergences were between *T. c. capensis* and *T. c. oatesi* (4.91%) and between *T. mossambicanus* and *T. usambaricus* (5.64%), suggesting very recent divergence or potentially conspecificity. Mean uncorrected pairwise sequence divergences for the ND4 dataset among *Thelotornis* lineages ranged from 4.55% to 11.94%. The ND4 results closely mirror that of cyt *b*, though with slight shifts in relative divergence values across some lineage pairs. The lowest divergence was between *T. c. capensis* and *T. c. oatesi* (4.55%), as in cyt *b*, supporting their close relationship and possible recent divergence. In contrast to *cyt b*, the divergence between *T. mossambicanus* and *T. usambaricus* was notably higher (7.61%), suggesting a more substantial evolutionary separation between these lineages than previously indicated. The most divergent lineage remained *T. kirtlandii*, with pairwise values of 10.38%–11.94% from other ingroup taxa.

Although cyt *b* sequence divergence suggests a closer relationship between *T. mossambicanus* and *T. usambaricus*, ND4 sequence divergence suggests that *T. mossambicanus* is genetically closer to *T. capensis sensu lato*. Overall, divergences among these lineages are modest (5.1%–7.6%), consistent with recent shared ancestry. In contrast, *X. uluguruensis* and *T. kirtlandii* consistently shows higher divergence values (9.5%–12.4% and >11.4%, respectively) from all other in-group taxa. Overall, the genetic distances and phylogenetic relationships reveal a hierarchical structure of divergence within *Thelotornis*, ranging from recent splits to deeply divergent clades consistent with independently evolving lineages.

For the STACEY Species Delimitation Analysis (SDA), lineage stability was quantified as the proportion of the posterior distribution of trees in which each focal lineage was consistently recovered within the same cluster. All seven focal lineages were recovered together as a single, distinct cluster with posterior probability = 1 under the multi-species coalescent framework implemented in STACEY (Species Tree And Classification Estimation; [47]). At lower posterior probabilities, a subset of three lineages (*T. mossambicanus*, *T. usambaricus* and *T.* sp.) occasionally formed their own cluster, though not supported. The overall signal across the posterior strongly supports recognition of all seven lineages as distinct evolutionary units (Figure 4B).

Haplotype networks constructed from cyt *b* sequences revealed strong concordance with species-level boundaries inferred from ASAP and genetic distances between taxa. Across the seven focal lineages of *Thelotornis* (including *X. uluguruensis*), each was recovered as distinct, with no haplotype sharing observed between lineages (Figure 4C). The number of unique haplotypes

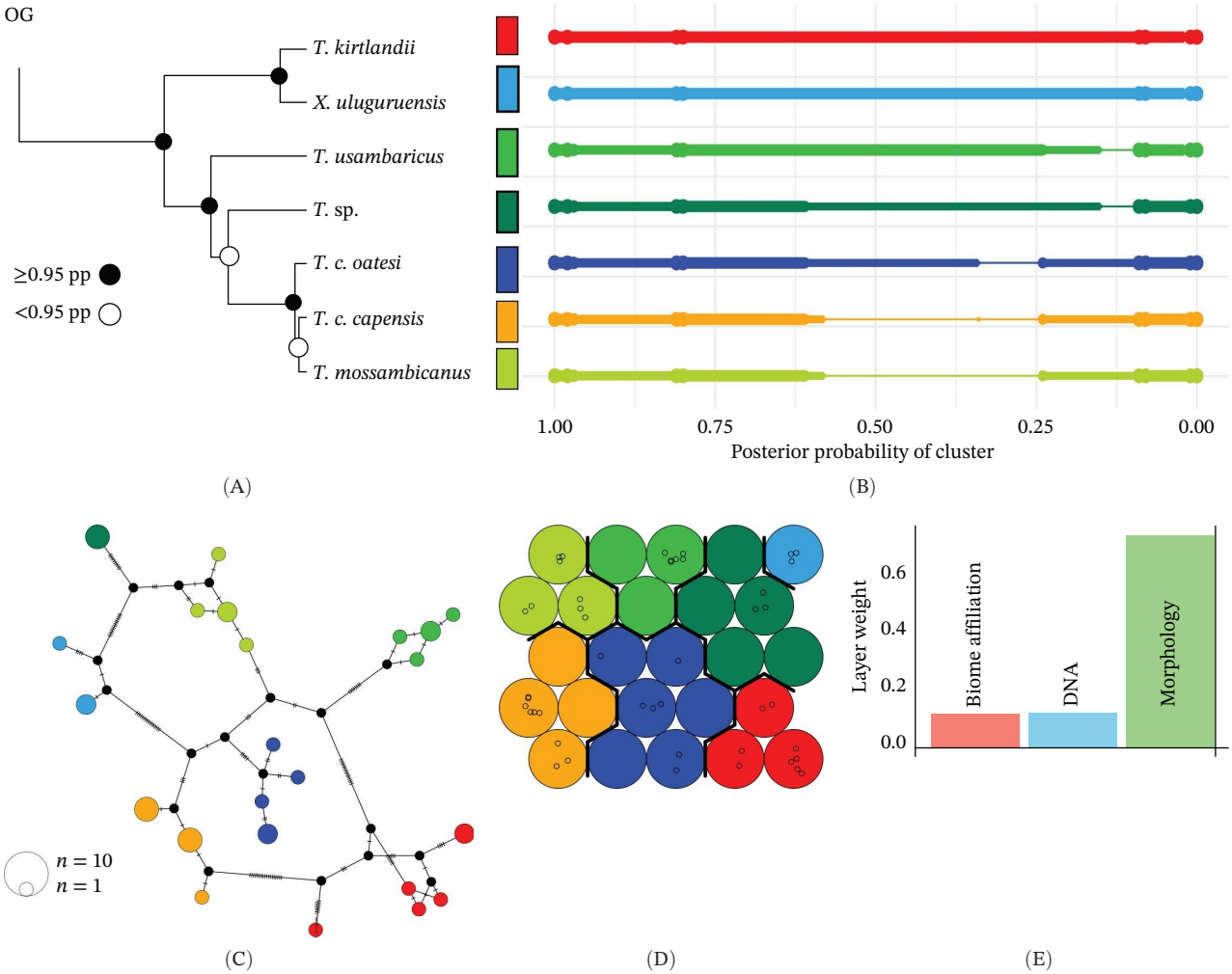

FIGURE 4 | Integrative delimitation of seven *Thelotornis* lineages. Multiple independent analytical approaches consistently recover the same seven distinct lineages. Colours are matched to terminal tips in the species tree (A) to aid visual comparison across panels. (A) ASAP barcode lineages are shown as coloured bars adjacent to the coalescent species tree (STACEY), which provides contextual support with posterior probabilities at nodes (black ≥0.95; white <0.95). (B) Lineage stability across SDA clustering replicates, with bar width indicating the proportion of posterior clusters in which each lineage is recovered as distinct. (C) Statistical parsimony cyt *b* haplotype network (POPART) showing no shared haplotypes among lineages, consistent with strong mitochondrial divergence and lack of recent gene flow. Circle size reflects haplotype frequency. (D) Unsupervised machine-learning analysis (SuperSOM) identifying seven discrete clusters congruent with the phylogenetic lineages; each hexagon represents a neurone in the SOM grid, coloured by lineage identity. (E) Relative contributions of data layers to the UML SuperSOM clustering, showing that morphology provides the strongest discriminatory signal, followed by biome affiliation and DNA data.

varied from one to five within each lineage, given the dataset (*T. kirtlandii* = 5, *T. usambaricus* = 4, *T.* sp. = 1, *T. mossambicanus* = 4, *T. c. capensis* = 3, *T. c. oatesi* = 4 and *X. uluguruensis* = 2), and several mutation steps and unsampled haplotypes exist between the seven lineages. Overall, the mitochondrial haplotype networks provide an independent, maternally inherited perspective that supports the distinctiveness of all seven lineages.

The UML SuperSOM models stabilised after 5000 iterations, indicating sufficient training of the SOM and robust cluster assignment (Supporting Information 4). When exploring the optimal number of $K = 2–10$ alongside assessing changes in total weighted sum of squares (WSS) across this range, we observed a distinct pattern in model fit, with the stability zone reached at $K = 7$. Clusters at $K = 7$ correspond with results from the barcoding species delimitation, as well as phylogenetic and morphological groupings, reinforcing its interpretation as the most biologically meaningful species delimitation scenario for *Thelotornis* (including *X. uluguruensis*; Figure 4D). Alternative clustering solutions ($K = 4–6$) shows partial concordance with morphology and geography, but conflated lineages that are not closely related, failing to preserve phylogenetic and biological distinctiveness. When the individual components of the UML SuperSOM are combined into three main data layers, that is, genetic, morphological and habitat affiliation, the morphological data layer appears to carry the strongest signal for lineage delineation and/or putative species clustering, while DNA and environmental data contribute equally to species delimitation when combined (Figure 4E). However, examination of the individual components within these three layers indicates that genetic data carries the strongest signal (Figure 4E and Supporting Information 4).

4 | Discussion

We present the first multilocus coalescent phylogeny of *Thelotornis*, integrating genetic, morphological and ecological data. Our analyses recover the genus, including *Xyelodontophis uluguruensis*, as monophyletic with a stem age of approximately 16.6 Mya, coinciding with the later phase of the Mid-Miocene climatic optimum [77–79]. African Vine Snake radiation appears to have been shaped by habitat fragmentation and varying ecological tolerances, facilitating persistence across forest, woodland and thicket habitats and ultimately giving rise to seven independently evolving, diagnosable species. Across all analyses, support for seven independently evolving lineages emerges from the congruence of multiple, partially independent data sources. Phylogenetic topology and divergence times provide a temporal framework, mitochondrial genetic distances (both bar-coding and mean uncorrected pairwise sequence divergences) and haplotype networks quantify lineage separation, and integrative UML SuperSOM clustering synthesises genetic, morphological and ecological information, with confidence in species limits arising from the convergence of these approaches despite known limitations of each method.

Although the stem of *Thelotornis* dates to the Mid-Miocene, the crown age indicates that diversification within the genus was delayed until the Late Miocene, *ca*. 8.3 Mya. A major split then separated a West–East African forest lineage, ancestral to *T. kirtlandii* and *X. uluguruensis*, from an East–Southern African lineage. This East–Southern African lineage subsequently gave rise to habitat generalists (*T. usambaricus*, *T.* sp., *T. mossambicanus* and *T. c. capensis*) as well as the savanna specialist *T. c. oatesi*. This diversification was likely shaped by Late-Miocene tectonic activity, fire regimes and aridification, which fragmented forests, promoted savanna expansion and facilitated southward dispersal of lineages [22].

The West–East African forest lineage of *Thelotornis*, emergence *ca*. 8 Mya, appears to have remained genetically cohesive through repeated episodes of habitat contraction, although some forest-associated lineages may have gone extinct, as documented in other Afrotropical taxa with comparable distributions and ages [80]. During Late-Miocene aridification between approximately 10 and 6.5 Mya, African tropical forests experienced abrupt and spatially heterogeneous losses, with substantial extinction across multiple forest clades [81, 82]. However, humid refugia persisted in topographically and climatically buffered regions, including the Eastern Arc and East African coastal forests [83]. These refugial areas likely enabled *Thelotornis* populations to persist while intervening populations were extirpated, with subsequent Pliocene humid phases temporarily reconnecting forest blocks and restoring limited gene flow [84, 85]. Renewed tectonic activity and global cooling during the Plio-Pleistocene, from approximately 3.6 to 1.4 Mya, further fragmented coastal and montane forests [22, 86], possibly isolating *T. kirtlandii* in lowland forests west of the Eastern Arc and *X. uluguruensis* in montane habitats by *ca*. 1.53 Mya, consistent with the Pliocene–Pleistocene forest refuge hypothesis [26, 87]. This long-term persistence, punctuated by habitat fragmentation, is reflected in mitochondrial genealogies: both species are separated from other lineages by multiple mutational steps, share no haplotypes and lack star-like topologies, suggesting prolonged population stability rather than recent demographic expansion. Although mitochondrial data capture only maternal histories, their concordance with multilocus phylogenetic structure supports long-standing isolation and refugial persistence.

The East–Southern African lineage diversified more rapidly during the early-mid Pliocene, giving rise to two Eastern African coastal species, *T. usambaricus* and *T.* sp. (*ca*. 5.5 and 4.5 Mya), which represent the first apparent habitat generalists within the genus. Fossil and isotopic evidence indicate that, in the Early–Mid Pliocene 'Golden Age', moist evergreen and semi-deciduous forests extended along the East African coast, facilitating dispersal into coastal forest–savanna mosaics [22, 83, 84]. From approximately 4 Mya onward, the progressive expansion of C_4-dominated ecosystems fragmented these humid forests into heterogeneous mosaics, a transitional phase during which the emergence of these lineages likely reflects ecological flexibility in response to increasingly seasonal and structurally complex habitats [88]. Subsequent East African Rift tectonics, Late-Pliocene aridification and sea-level fluctuations *ca*. 2.7 Mya further subdivided coastal forests, potentially isolating *T. usambaricus* in northern regions and *T.* sp. farther south. Persistence of ancestral populations in southern Tanzanian coastal forests may have enabled colonisation of Vamizi Island off the north coast of Mozambique during Pleistocene lowstands, given the short mainland distance of approximately 4 km and the island's patch reef structure [89, 90], although rare rafting events cannot be excluded [91–93]. This scenario does not require persistence of the founding population to the present day and is equally compatible with subsequent local extirpation, undetected persistence or absorption into the broader southern mainland radiation. In addition, a secondary island-to-mainland colonisation cannot be excluded. Such a model would require multiple dispersal and recolonisation events and is therefore not favoured relative to a simple mainland-to-island colonisation scenario, especially given that phylogenetic topology does not resolve directionality and the Vamizi lineage predates diversification of the southern mainland clade. Nonetheless, the resulting insular lineage is genetically distinct and indicates a strong founder effect, represented by a single haplotype separated from mainland lineages by several mutational steps with no intermediates, consistent with isolation following Pleistocene colonisation rather than very recent dispersal.

Although temporal estimates broadly align with patterns observed across deeper squamate evolutionary timescales (e.g., [18]), limited nuclear sampling warrants caution when interpreting species boundaries and divergence timing at finer phylogenetic resolution. For example, the youngest diversification within *Thelotornis* gave rise to *T. mossambicanus*, *T. c. capensis* and *T. c. oatesi*, which have persisted since *ca*. 0.67 Mya. These lineages occupy distinct, but parapatric ecological settings: *T. mossambicanus* occurs across a relatively broad expanse of East–Southern coastal–lowland mosaics, *T. c. capensis* is restricted to southern coastal thicket habitats and *T. c. oatesi* specialises in open savanna, a pattern consistent with the establishment of C_4 grasslands by *ca*. 1 Mya [7, 88, 94]. Against this ecological backdrop, signatures of incomplete lineage sorting (ILS) may be evident, potentially reflecting gradual separation within heterogeneous coastal, thicket and savanna mosaics, as suggested by phylogenetic inference methods. Consistent with this interpretation, the mitochondrial genealogy resolves distinct lineages separated by relatively few mutational steps, while barcoding indicates that taxa remain diagnosable despite low uncorrected sequence divergence. However, these patterns are comparable to

shallow nuclear divergence observed in other young radiations [95], which also reflect ongoing lineage sorting rather than complete isolation. In this context, and in accordance with the USC adopted here, the observed signatures of ILS are interpreted as an early stage of divergence, particularly in clinal or ecotonal settings where barriers to gene flow arise gradually [29].

Overall, the observed patterns of lineage differentiation in *Thelotornis* are most parsimoniously interpreted as biologically meaningful divergence rather than methodological artefacts. This interpretation is supported by the concordance among genetic, morphological and ecological lines of evidence, reducing the risk of both over- and under-splitting and yielding more defensible taxonomic inferences [66, 96, 97]. Within this integrative framework, each analytical approach contributes complementary and partially independent insights but also imposes distinct limitations. Phylogenetic inference and coalescent models provide temporal and relational structure but remain sensitive to marker sampling and ILS. Mitochondrial genealogies capture lineage separation and historical isolation yet reflect only maternal histories. Morphological data offer discriminatory power that is contingent on the number and selection of measured variables. The UML SuperSOM integrates multiple data types while remaining dependent on data composition and scaling. Species boundaries are therefore inferred from patterns of concordance across methods rather than from any single analytical outcome. Similar patterns of biome-associated diversification have been documented in other African reptiles, including arboreal colubrids, indicating that arboreality and the capacity for range expansion may consistently shape lineage divergence across comparably structured landscapes [14, 24, 25, 98].

Morphological characters for *Thelotornis* species correspond closely to evolutionary relationships (e.g., *X. uluguruensis*–*T. kirtlandii* and *T. mossambicanus*–*T. c. capensis*–*T. c. oatesi*), in contrast to many colubrid genera where morphology often poorly reflects genetic divergence [14, 99–101]. These hierarchical patterns suggest that certain traits diversified alongside lineages, potentially reflecting functional adaptations associated with arboreality, including visual and locomotory demands [1–3, 102]. Morphological diversification along lineages is further clarified when considered in the context of habitat affiliation use, highlighting both evolutionary resilience and conservation implications. For example, *T. kirtlandii*, previously thought to range broadly from West to East Africa, may in fact be restricted to lowland forest and mangrove habitats east of the Albertine Rift, with reported populations in Tanzanian montane habitats likely representing misidentifications of *X. uluguruensis* or *T. usambaricus* (Massisiswi, Udzungwa Mountains and Pasagulu) [8, 13, 103]. In turn, *X. uluguruensis* occupies a wider distribution extending beyond the Uluguru Mountains into South–Eastern Tanzania, including the Udzungwa Mountains, where it remains associated with montane forest, while *T. usambaricus*, originally described as a coastal forest specialist, inhabits a broader array of habitats, including mangroves, miombo woodlands, bushland and thicket [8, 13].

The concordance among morphology, ecology and multilocus genetic evidence provides a robust basis for taxonomic inference within *Thelotornis*, largely building on previously described species, with the exception of *T.* sp. from Vamizi Island, Mozambique, which represents an undescribed lineage (Farooq et al. in prep.). Based on these lines of evidence, we formally recognise seven species: *T. kirtlandii*, *T. uluguruensis* comb. nov., *T. usambaricus*, *T.* sp, *T. mossambicanus* and two taxa formerly treated as subspecies of *T. capensis*, here elevated to species rank as *T. capensis* and *T. oatesi* stat. nov. In conjunction with these taxonomic updates, we amend the diagnosis of *Thelotornis* to include a rounded pupil and strongly curved rear maxillary teeth with sharp anterior and posterior flanges and a narrow base, as exemplified by *T. uluguruensis*. Collectively, *Thelotornis* appear to form a monophyletic, relatively young radiation, likely influenced by historical climate change and habitat fragmentation. Improved geographic coverage and targeted investigation of possible ecomorphological adaptations will be essential to further elucidate how habitat structure drives functional and ecological divergence among African Vine Snakes.

Author Contributions

Conceived and designed the analysis, data analyses, results interpretation: Hanlie M. Engelbrecht and Kutloano L. Seeiso. Data acquisition: Hanlie M. Engelbrecht, Kutloano L. Seeiso and Werner A. Conradie. Writing and editing: Hanlie M. Engelbrecht and Werner A. Conradie. Validation: all authors.

Acknowledgments

Field work in Mozambique was carried out under the permission by the Direcção Provincial da Agricultura (Nampula and Zambezia provinces, Mozambique) with export permission granted by the Museu de Historia Natural (315/MHN/E.27/2014) and CapeNature import permit 0045-AAA007-00217. We thank the Wild Bird Trust, which administers the National Geographic Okavango Wilderness Project (2015–2019 National Geographic Society grant). Angolan material was collected and exported under the following permits issued by MINAMB: 31/GGPCC/2016 and 151/INBAC/MINAMB/2019. This work was supported financially and logistically by several institutions as follows: the National Geographic Society Committee for Research and Exploration (Grant CRE 9281-13), the South African National Biodiversity Institute (SANBI) (grant held by Krystal A. Tolley) and the National Research Foundation of South Africa (NRF) (Grants #92776 and #129835), which funded the 2014 Mozambique survey, fieldwork logistics, laboratory resources, sequencing and analytical pipelines, with additional logistical support for fieldwork in 2014 provided by Khangela Safaris. We would also like to take this opportunity to thank the following individuals for their assistance in the field and sample collection: Beryl Wilson, Buyisile Makhubo, Colin Tilbury, Gabriella Bittencourt-Silva; Gary Nicolau, Luke Verburgt, Krystal Tolley, Pedro vaz Pinto, Thomas Branch, Simon Loader, William R. Branch and Götz Neef.

Funding

This work was supported financially and logistically by several institutions as follows: the National Geographic Society Committee for Research and Exploration (Grant CRE 9281-13), the South African National Biodiversity Institute (SANBI) (grant held by Krystal A. Tolley) and the National Research Foundation of South Africa (NRF) (Grants #92776 and #129835), which funded the 2014 Mozambique survey, fieldwork logistics, laboratory resources, sequencing and analytical pipelines, with additional logistical support for fieldwork in 2014 provided by Khangela Safaris.

Disclosure

This research was carried out independently, without influence from external funding sources or personal relationships. All findings and interpretations reported here are solely the product of the authors' academic investigation.

Ethics Statement

All research protocols in this study were conducted with approved ethical clearance from the Animal Research Ethics Committee (AREC) and University of the Witwatersrand (Waiver 19-04-2022-O).

Conflicts of Interest

The authors declare no conflicts of interest.

Data Availability Statement

The data that support the findings of this study are available in the supporting information of this article.

References

1. L. Pizzatto, S. M. Almeida-Santos, and R. Shine, "Life-History Adaptations to Arboreality in Snakes," *Ecology* 88, no. 2 (2007): 359–366.

2. Z. Tadić, "Snakes: Slithering From Sensory Physiology to Cognition," *Comparative Cognition & Behavior Reviews* 18 (2023): 95–120.

3. D. Hudry and A. Herrel, "Divergent Paths, Convergent Heads: Morphological Adaptation of Head Shape to Ecological Niches in Snakes," bioRxiv, 2025-05 (2025).

4. A. Figueroa, A. D. McKelvy, L. L. Grismer, C. D. Bell, S. P. Lailvaux, and A. Parmakelis, "A Species-Level Phylogeny of Extant Snakes With Description of a New Colubrid Subfamily and Genus," *PLoS ONE* 11, no. 9 (2016): e0161070.

5. H. Zaher, R. W. Murphy, J. C. Arredondo, et al., "Large-Scale Molecular Phylogeny, Morphology, Divergence-Time Estimation, and the Fossil Record of Advanced Caenophidian Snakes (Squamata: Serpentes)," *PLoS ONE* 14, no. 5 (2019): e0217959.

6. M. Bourgeois, "Contribution à la Morphologie Comparée du Crâne des Ophidiens de l'Afrique Centrale," Publications de l'Université Officielle du Congo à Lubumbashi (1968): 1–293.

7. D. G. Broadley, "Problems Presented by Geographical Variation in the African Vine Snakes, Genus *Thelotornis*," *South African Journal of Zoology* 14, no. 3 (1979): 125–131.

8. D. G. Broadley, "A Review of the Genus *Thelotornis* A. Smith in Eastern Africa, With the Description of a New Species From the Usambara Mountains (Serpentes: Colubridae: Dispholidini)," *African Journal of Herpetology* 50, no. 2 (2001): 53–70.

9. D. Broadley and H. Farooq, "Geographical Distributions: *Thelotornis usambaricus*," *African Herp News* 59 (2013): 48–50.

10. S. Spawls, K. Howell, H. Hinkel, and M. Menegon, "Field Guide to East African Reptiles," (Bloomsbury Publishing, United Kingdom, 2018).

11. D. Pietersen, L. Verburgt, and J. Davies, *Snakes and Other Reptiles of Zambia and Malawi* (Penguin Random House South Africa, 2021).

12. J. Marais, "A Complete Guide to the Snakes of Southern Africa," in *South Africa: Penguin Random House South Africa*, (Struik Nature, (An Imprint of Penguin Random House South Africa (Pty) Ltd), 2022).

13. D. G. Broadley and V. Wallach, "Review of the Dispholidini, With the Description of a New Genus and Species From Tanzania (Serpentes, Colubridae)," *Bulletin of the Natural History Museum: Zoology Series* 68, no. 2 (2002): 57–74.

14. H. M. Engelbrecht, W. R. Branch, E. Greenbaum, et al., "Diversifying Into the Branches: Species Boundaries in African Green and Bush Snakes, Philothamnus (Serpentes: Colubridae)," *Molecular Phylogenetics and Evolution* 130 (2019): 357–365.

15. J. F. Trape, B. Hughes, M. Collet, and O. Mediannikov, "Phylogénie moléculaire des serpents du groupe Philothamnus heterodermus (Hallowell, 1857)(Squamata: Colubridae: Colubrinae) avec la description de deux espèces nouvelles," *Bulletin de la Société Herpétologique de France* 31, no. 179 (2022): 27–42.

16. E. Greenbaum, O. S. Pauwels, V. Gvoždík, et al., "Systematics of the Thirteen-Scaled Green Snake *Philothamnus carinatus* (Squamata: Colubridae), With the Description of a Cryptic New Species From Central and East Africa," *African Journal of Herpetology* 72, no. 2 (2023): 119–144.

17. T. G. Eimermacher, *Phylogenetic Systematics of Dispholidine Colubrids (Serpentes: Colubridae)*, (Doctoral Dissertation, University of Texas at Arlington, 2012).

18. Y. Zheng and J. J. Wiens, "Combining Phylogenomic and Supermatrix Approaches, and a Time-Calibrated Phylogeny for Squamate Reptiles (Lizards and Snakes) Based on 52 Genes and 4162 Species," *Molecular Phylogenetics and Evolution* 94 (2016): 537–547.

19. R. Bobe, "The Evolution of Arid Ecosystems in Eastern Africa," *Journal of Arid Environments* 66, no. 3 (2006): 564–584.

20. R. Bobe, V. Aldeias, Z. Alemseged, et al., "The First Miocene Fossils From Coastal Woodlands in the Southern East African Rift," *iScience* 26, no. 9 (2023): 107644.

21. Y. Miao, J. Nie, X. Hu, et al., "Wildfire History and Savanna Expansion Across Southern Africa Since the Late Miocene," *Palaeogeography, Palaeoclimatology, Palaeoecology* 603 (2022): 111189.

22. T. L. P. Couvreur, G. Dauby, A. Blach-Overgaard, et al., "Tectonics, Climate and the Diversification of the Tropical African Terrestrial Flora and Fauna," *Biological Reviews* 96, no. 1 (2021): 16–51.

23. W. D. Kissling, A. Blach-Overgaard, R. E. Zwaan, and P. Wagner, "Historical Colonization and Dispersal Limitation Supplement Climate and Topography in Shaping Species Richness of African Lizards (Reptilia: Agaminae)," *Scientific Reports* 6, no. 1 (2016): 34014.

24. H. P. Linder, H. M. de Klerk, J. Born, N. D. Burgess, J. Fjeldså, and C. Rahbek, "The Partitioning of Africa: Statistically Defined Biogeographical Regions in Sub-Saharan Africa," *Journal of Biogeography* 39, no. 7 (2012): 1189–1205.

25. H. M. Engelbrecht, W. R. Branch, and K. A. Tolley, "Snakes on an African Plain: The Radiation of *Crotaphopeltis* and *Philothamnus* Into Open Habitat (Serpentes: Colubridae)," *PeerJ* 9 (2021): e11728.

26. B. O. Ogolowa, A. Brelsford, J. Fjeldså, et al., "Plio-Pleistocene Climatic Fluctuations and Divergence With Gene Flow Drive Continent-Wide Diversification in an African Bird," *Molecular Ecology* 34, no. 10 (2025): e17770.

27. J. J. Wiens, "Speciation Across Life and the Origins of Biodiversity Patterns," *Evolutionary Journal of the Linnean Society* 3, no. 1 (2024): kzae025.

28. K. De Queiroz, "Species Concepts and Species Delimitation," *Systematic Biology* 56, no. 6 (2007): 879–886.

29. K. De Queiroz, "Recent Developments in Species Delimitation and Taxonomy Considered in the Context of the Unified Species Concept," *Herpetologica* 81, no. 2 (2025): 95–103.

30. B. P. Noonan and P. T. Chippindale, "Dispersal and Vicariance: The Complex Evolutionary History of Boid Snakes," *Molecular Phylogenetics and Evolution* 40, no. 2 (2006): 347–358.

31. R. Lawson, J. B. Slowinski, B. I. Crother, and F. T. Burbrink, "Phylogeny of the Colubroidea (Serpentes): New Evidence From Mitochondrial and Nuclear Genes," *Molecular Phylogenetics and Evolution* 37, no. 2 (2005): 581–601.

32. F. T. Burbrink, R. Lawson, and J. B. Slowinski, "Mitochondrial DNA Phylogeography of the Polytypic North American Rat Snake (Elaphe Obsoleta): A Critique of the Subspecies Concept," *Evolution* 54, no. 6 (2000): 2107–2118.

33. S. R. Palumbi, "Nucleic Acids II: the Polymerase Chain Reaction," in *Molecular Systematics*, eds. D. M. Hillis, C. Moritz, and B. K. Mable, (Sinauer Associates, Inc., 1996): 205–247.

34. E. Arévalo, S. K. Davis, and J. W. Sites, "Mitochondrial DNA Sequence Divergence and Phylogenetic Relationships Among Eight Chromosome Races of the Sceloporus Grammicus Complex (Phrynosomatidae) in Central Mexico," *Systematic Biology* 43, no. 3 (1994): 387–418.

35. C. E. Pook, U. Joger, N. Stümpel, and W. Wüster, "When Continents Collide: Phylogeny, Historical Biogeography and Systematics of the Medically Important Viper Genus Echis (Squamata: Serpentes: Viperidae)," *Molecular Phylogenetics and Evolution* 53, no. 3 (2009): 792–807.

36. M. MacManes, "MacManes Salt Extraction Protocol," *Journal Contribution* (2013).

37. K. Tamura, G. Stecher, and S. Kumar, "MEGA11: Molecular Evolutionary Genetics Analysis Version 11, Version 12 for Adaptive and Green Computing," *Molecular Biology and Evolution, Molecular Biology and Evolution* 41, no. 12 (2021), 3027, 2024.

38. D. C. Main, J. M. Taft, A. J. Geneva, B. J. Vuuren, and K. A. Tolley, "The Efficacy of Single Mitochondrial Genes at Reconciling the Complete Mitogenome Phylogeny—A Case Study on Dwarf Chameleons," *PeerJ* 12 (2024): e17076.

39. O. Chernomor, A. von Haeseler, and B. Q. Minh, "Terrace Aware Data Structure for Phylogenomic Inference From Supermatrices," *Systematic Biology* 65, no. 6 (2016): 997–1008.

40. S. Kalyaanamoorthy, B. Q. Minh, T. K. F. Wong, A. von Haeseler, and L. S. Jermiin, "ModelFinder: Fast Model Selection for Accurate Phylogenetic Estimates," *Nature Methods* 14, no. 6 (2017): 587–589.

41. D. T. Hoang, O. Chernomor, A. von Haeseler, B. Q. Minh, and L. S. Vinh, "UFBoot2: Improving the Ultrafast Bootstrap Approximation," *Molecular Biology and Evolution* 35, no. 2 (2018): 518–522.

42. B. Q. Minh, M. A. T. Nguyen, and A. von Haeseler, "Ultrafast Approximation for Phylogenetic Bootstrap," *Molecular Biology and Evolution* 30, no. 5 (2013): 1188–1195.

43. B. Q. Minh, H. A. Schmidt, O. Chernomor, et al., "IQ-TREE. 2: New Models and Efficient Methods for Phylogenetic Inference in the Genomic Era," *Molecular Biology and Evolution* 37, no. 5 (2020): 1530–1534.

44. B. Q. Minh, R. Lanfear, NL-T. J. Trifinopoulos, D. Schrempf, and H. A. Schmidt, "IQ-TREE Version 2.2.0: Tutorials and Manual Phylogenomic Software by Maximum Likelihood," (2022).

45. S. Guindon, J.-F. Dufayard, V. Lefort, M. Anisimova, W. Hordijk, and O. Gascuel, "New Algorithms and Methods to Estimate Maximum-Likelihood Phylogenies: Assessing the Performance of PhyML 3.0," *Systematic Biology* 59, no. 3 (2010): 307–321.

46. R. Bouckaert, T. G. Vaughan, J. Barido-Sottani, et al., "BEAST. 2.5: An Advanced Software Platform for Bayesian Evolutionary Analysis," *PLoS Computational Biology* 15, no. 4 (2019): e1006650.

47. G. Jones, "Algorithmic Improvements to Species Delimitation and Phylogeny Estimation Under the Multispecies Coalescent," *Journal of Mathematical Biology* 74, no. 1-2 (2017): 447–467.

48. A. J. Drummond, G. K. Nicholls, A. G. Rodrigo, and W. Solomon, "Estimating Mutation Parameters, Population History and Genealogy Simultaneously From Temporally Spaced Sequence Data," *Genetics* 161, no. 3 (2002): 1307–1320.

49. A. J. Drummond, S. Y. W. Ho, M. J. Phillips, A. Rambaut, and D. Penny, "Relaxed Phylogenetics and Dating With Confidence," *PLoS Biology* 4, no. 5 (2006): e88.

50. Z. T. Nagy, U. Joger, M. Wink, F. Glaw, and M. Vences, "Multiple Colonization of Madagascar and Socotra by Colubrid Snakes: Evidence From Nuclear and Mitochondrial Gene Phylogenies," *Proceedings of the Royal Society of London. Series B: Biological Sciences* 270, no. 1533 (2003): 2613–2621.

51. M. Ivanov, "The Oldest Known Miocene Snake Fauna From Central Europe: Merkur-North Locality, Czech Republic," *Acta Palaeontologica Polonica* 47 (2002): 513–534.

52. A. Rambaut and A. J. Drummond, "TreeAnnotator v. 2.3.0. Part of the BEAST Package," (2014).

53. A. Rambaut, A. J. Drummond, D. Xie, G. Baele, M. A. Suchard, and E. Susko, "Posterior Summarization in Bayesian Phylogenetics Using Tracer 1.7," *Systematic Biology* 67, no. 5 (2018): 901–904.

54. A. J. Drummond and A. Rambaut, "BEAST: Bayesian Evolutionary Analysis by Sampling Trees," *BMC Evolutionary Biology* 7, no. 1 (2007): 214.

55. N. Puillandre, S. Brouillet, and G. Achaz, "ASAP: Assemble Species by Automatic Partitioning," *Molecular Ecology Resources* 21, no. 2 (2021): 609–620.

56. S. Kumar, G. Stecher, M. Suleski, et al., "MEGA12: Molecular Evolutionary Genetic Analysis Version 12 for Adaptive and Green Computing," *Molecular Biology and Evolution* 41, no. 12 (2024): 1–9.

57. J. W. Leigh, D. Bryant, and S. Nakagawa, "POPART: Full-Feature Software for Haplotype Network Construction," *Methods in Ecology and Evolution* 6, no. 9 (2015): 1110–1116.

58. J. Rozas, A. Ferrer-Mata, J. C. Sánchez-DelBarrio, et al., "DnaSP. 6: DNA Sequence Polymorphism Analysis of Large Data Sets," *Molecular Biology and Evolution* 34, no. 12 (2017): 3299–3302.

59. E. Paradis, J. Claude, and K. Strimmer, "APE: Analyses of Phylogenetics and Evolution in R Language," *Bioinformatics* 20, no. 2 (2004): 289-290.

60. K. P. Schliep, "Phangorn: Phylogenetic Analysis in R," *Bioinformatics* 27, no. 4 (2011): 592-593.

61. H. Wickham, R. François, L. Henry, K. Müller, and D. Vaughan, "dplyr: A Grammar of Data Manipulation (Version 1.1.4) [R Package]," 2023, https://CRAN.R-project.org/package=dplyr.

62. H. Wickham, D. Vaughan, and M. Girlich, 2024, tidyr: Tidy messy data (Version 1.3.1) [R package] https://CRAN.R-project.org/package=tidyr.

63. H. Wickham, "Stringr: Simple, Consistent Wrappers for Common String Operations (Version 1.5.1) [R Package]," 2023, https://CRAN.R-project.org/package=stringr.

64. H. Wickham, *ggplot2: Elegant Graphics for Data Analysis* (Springer-Verlag, 2016).

65. H. Wickham, J. Hester, and J. Bryan, "readr: Read Rectangular Text Data (Version 2.1.5) [R Package]," 2024, https://CRAN.R-project.org/package=readr.

66. R. A. Pyron, "Unsupervised Machine Learning for Species Delimitation, Integrative Taxonomy, and Biodiversity Conservation," *Molecular Phylogenetics and Evolution* 189 (2023): 107939.

67. D. M. Olson, E. Dinerstein, E. D. Wikramanayake, et al., "Terrestrial Ecoregions of the World: A New Map of Life on Earth," *BioScience* 51, no. 11 (2001): 933–938.

68. R. Core Team, *R: A Language and Environment for Statistical Computing* (R Foundation for Statistical Computing, Vienna, 2022, https://www.R-project.org.

69. E. Paradis, K. Schliep, and R. Schwartz, "ape 5.0: An Environment for Modern Phylogenetics and Evolutionary Analyses in R," *Bioinformatics* 35, no. 3 (2019): 526–528.

70. R. Wehrens and L. M. C. Buydens, "Self- and Super-Organizing Maps in *R*: The Kohonen Package," *Journal of Statistical Software* 21, no. 5 (2007): 1–19.

71. A. Kassambara and F. Mundt, "factoextra: Extract and Visualize the Results of Multivariate Data Analyses (Version 1.0.7) [R Package]," 2020, https://CRAN.R-project.org/package=factoextra.

72. M. Maechler, P. Rousseeuw, A. Struyf, M. Hubert, and K. Hornik, "Cluster: Cluster Analysis Basics and Extensions (Version 2.1.6) [R Package]," (2023).

73. L. J. P. van der Maaten and G. E. Hinton, "Visualizing High-Dimensional Data Using t-SNE," *Journal of Machine Learning Research* 9 (2008): 2579–2605.

74. L. J. P. van der Maaten, "Accelerating t-SNE Using Tree-Based Algorithms," *Journal of Machine Learning Research* 15 (2014): 3221–3245.

75. J. H. Krijthe, "Rtsne: T-Distributed Stochastic Neighbor Embedding Using a Barnes-Hut Implementation [R Package]," 2015, https://github.com/jkrijthe/Rtsne.

76. M. Charrad, N. Ghazzali, V. Boiteau, and A. Niknafs, "NbClust: An *R* Package for Determining the Relevant Number of Clusters in a Data Set," *Journal of Statistical Software* 61, no. 6 (2014): 1–36, 2014, http://www.jstatsoft.org/v61/i06/.

77. M. Gürsoy, "Bivalvia Biostratigraphy of Aksütlü Region (Hekimhan, NW Malatya, Türkiye) and Paleoclimatological Interpretations," *Bulletin of the Mineral Research and Exploration* 177, no. 177 (2025): 1-2.

78. K. Methner, M. Campani, J. Fiebig, N. Löffler, O. Kempf, and A. Mulch, "Middle Miocene Long-Term Continental Temperature Change in and Out of Pace With Marine Climate Records," *Scientific Reports* 10, no. 1 (2020): 7989.

79. J. A. McCartney, S. N. Bouchard, J. A. Reinhardt, et al., "The Oldest Lamprophiid (Serpentes, Caenophidia) Fossil From the Late Oligocene Rukwa Rift Basin, Tanzania and the Origins of African Snake Diversity," *Geobios* 66-67 (2021): 67–75.

80. O. Hagen, A. Skeels, R. E. Onstein, W. Jetz, and L. Pellissier, "Earth History Events Shaped the Evolution of Uneven Biodiversity Across Tropical Moist Forests," *Proceedings of the National Academy of Sciences* 118, no. 40 (2021): e2026347118.

81. L.-P. M. J. Dagallier, F. L. Condamine, and T. L. P. Couvreur, "Sequential Diversification With Miocene Extinction and Pliocene Speciation Linked to Mountain Uplift Explains the Diversity of the African Rain Forest Clade Monodoreae (Annonaceae)," *Annals of Botany* 133, no. 5-6 (2024): 677–696.

82. B. Brée, A. J. Helmstetter, K. Bethune, J.-P. Ghogue, B. Sonké, and T. L. P. Couvreur, "Diversification of African Rainforest Restricted Clades: Piptostigmateae and Annickieae (Annonaceae)," *Diversity* 12, no. 6 (2020): 227.

83. J. C. A. Joordens, C. S. Feibel, H. B. Vonhof, A. S. Schulp, and D. Kroon, "Relevance of the Eastern African Coastal Forest for Early Hominin Biogeography," *Journal of Human Evolution* 131 (2019): 176–202.

84. R. Bonnefille, "Cenozoic Vegetation, Climate Changes and Hominid Evolution in Tropical Africa," *Global and Planetary Change* 72, no. 4 (2010): 390–411.

85. U. Ring, "Tectonic Dynamics in the African Rift Valley and Climate Change," in *Oxford Research Encyclopedia of Climate Science*, (Oxford University Press, 2018).

86. M. A. Maslin, C. M. Brierley, A. M. Milner, S. Shultz, M. H. Trauth, and K. E. Wilson, "East African Climate Pulses and Early Human Evolution," *Quaternary Science Reviews* 101 (2014): 1–17.

87. M. Ernst, M.-O. Rödel, and M. P. K. Blom, "Towards a Comprehensive View on Evolutionary Refugia in West African Rainforests," *Frontiers of Biogeography* 18 (2025): e139537.

88. T. Caley, A. Souron, K. T. Uno, and G. A. Macho, "Climate and Human Evolution: Insights From Marine Records," *Annual Review of Marine Science* 17, no. 1 (2025): 23–53.

89. J. Garnier, I. Silva, J. Davisdson, N. Hill, L. Muaves, et al., "Co-Management of the Reef at Vamizi Island, Northern Mozambique," Ten Years After Bleaching –Facing the Consequences of Climate Change in the Indian Ocean. p. 121–128 Mombasa: CORDIO Status Report, Coastal Oceans Research and Development in the Indian Ocean/Sida-SAREC (2008).

90. N. O. Hill, J. Davidson, I. Silva, et al., "Coral and Reef Fish in the Northern Quirimbas Archipelago, Mozambique—A First Assessment," *Western Indian Ocean Journal of Marine Science* 8, no. 1 (2009).

91. K. A. Tolley, T. M. Townsend, and M. Vences, "Large-Scale Phylogeny of Chameleons Suggests African," (2013).

92. T. M. Townsend, K. A. Tolley, F. Glaw, W. Böhme, and M. Vences, "Eastward From Africa: Palaeocurrent-Mediated Chameleon Dispersal to the Seychelles Islands," *Biology Letters* 7, no. 2 (2011): 225–228.

93. A. Čerňanský, A. Herrel, J. M. Kibii, C. V. Anderson, R. Boistel, and T. Lehmann, "The Only Complete Articulated Early Miocene Chameleon Skull (Rusinga Island, Kenya) Suggests an African Origin for Madagascar's Endemic Chameleons," *Scientific Reports* 10, no. 1 (2020): 109.

94. D. Fidalgo, A. Rosas, V. Vizcaíno-Varo, C. Tornero, and J. Madurell-Malapeira, "New Evidence for the Distribution of C3-C4 Grasslands Throughout the Quaternary From Stable Isotope Analysis in Hippopotamuses," *Spanish Journal of Palaeontology* (2025).

95. D. P. Toews and A. Brelsford, "The Biogeography of Mitochondrial and Nuclear Discordance in Animals," *Molecular Ecology* 21, no. 16 (2012): 3907–3930.

96. J. Villamil, M. Morando, L. J. Avila, et al., "Revisiting the Multispecies Coalescent Model Fit With an Example From a Complete Molecular Phylogeny of the *Liolaemus wiegmannii* Species Group (Squamata: Liolaemidae)," *Systematic Biology* (2025): syaf048.

97. F. T. Burbrink, E. A. Myers, and R. A. Pyron, "Understanding Species Limits Through the Formation of Phylogeographic Lineages," *Ecology and Evolution* 14, no. 10 (2024): e70263.

98. P. Li and J. J. Wiens, "What Drives Diversification? Range Expansion Tops Climate, Life History, Habitat and Size in Lizards and Snakes," *Journal of Biogeography* 49, no. 2 (2022): 237–247.

99. J. C. Murphy, S. P. Charles, R. M. Lehtinen, and K. L. Koeller, "A Molecular and Morphological Characterization of Oliver's Parrot Snake, *Leptophis coeruleodorsus* (Squamata: Serpentes: Colubridae) With the Description of a New Species From Tobago," *Zootaxa* 3718, no. 6 (2013): 561–574.

100. H. M. Engelbrecht, W. R. Branch, E. Greenbaum, M. Burger, W. Conradie, and K. A. Tolley, "African Herald Snakes, *Crotaphopeltis*, Show Population Structure for a Widespread Generalist but Deep Genetic Divergence for Forest Specialists," *Journal of Zoological Systematics and Evolutionary Research* 58, no. 4 (2020): 1220–1233.

101. R. C. Jadin, C. Blair, S. A. Orlofske, et al., "Not Withering on the Evolutionary Vine: Systematic Revision of the Brown Vine Snake (Reptilia: Squamata: Oxybelis) From Its Northern Distribution," *Organisms Diversity & Evolution* 20, no. 4 (2020): 723–746.

102. H. C. Astley and B. C. Jayne, "Effects of Perch Diameter and Incline on the Kinematics, Performance and Modes of Arboreal Locomotion of Corn Snakes (*Elaphe guttata*)," *Journal of Experimental Biology* 210, no. 21 (2007): 3862–3872.

103. G. C. Akani, L. U. C. A. Luiselli, and F. M. Angelici, "Diet of *Thelotornis kirtlandii* (Serpentes: Colubridae: Dispholidini) From Southern Nigeria," *Herpetological Journal* 12, no. 4 (2002): 179–182.

Supporting Information

Additional supporting information can be found online in the Supporting Information section.

Supporting Information 1. Sample information for *Thelotornis*, including specimen IDs, voucher numbers, localities, and GenBank accession numbers. Specimen ID numbers correspond to DNA field numbers, which indicate the collector as follows: BHMP = Buyisile Makhubo and Hanlie M. Engelbrecht (Mpumalanga); BILL, NR = William R. Branch; CMRK = Chris Kelley; CT = Colin Tilbury; EI = Luke Verburgt (Enviro-Insight cc.);

GNK = Gary Nicolau; KT, MOZ = Krystal Tolley; MBUR = Marius Burger; PVP = Pedro Vaz Pinto; TGE = Thomas Eimermacher; TB = Thomas Branch; WC = Werner Conradie; WW = Wolfgang Wüster; CRT = TBA. Voucher numbers indicate museum catalogue numbers: IPMP = Institute of Pharmacy and Molecular Biotechnology; MTSN = Museo Tridentino di Scienze Naturali; PEM = Port Elizabeth Museum; USNM = United States National Museum; UTEP = University of Texas at El Paso Biodiversity Collections; YPM = Yale Peabody Museum. NA indicates missing information.

Supporting Information 2. BEAST 2 XML input file for coalescent-based species tree inference, lineage diversification and downstream species delimitation using STACEY and the STACEY Species Delimitation Analyser. The file includes sequence alignments, taxon assignments, coalescent tree priors for species tree inference, and STACEY-specific settings for Bayesian inference of lineage diversification and species boundaries. This input file was used for six independent runs, each initiated with a different random seed.

Supporting Information 3. Maximum likelihood trees inferred using IQ-TREE. (A) Dataset 1: c-mos + NT3 + cyt *b* + ND4. (B) Dataset 2: mitochondrial loci cyt *b* + ND4. These trees include all sampled individuals with their corresponding field numbers as tip labels. Node support is represented as SH-aLRT/UFBoot values, with strong support defined as SH-aLRT ≥80% and UFBoot ≥95%. Branch lengths are scaled to the number of substitutions per site.

Supporting Information 4. Unsupervised machine-learning (UML) SuperSOM analyses of *Thelotornis* lineages. Panels show the SuperSOM training process and outputs used for integrative lineage delimitation. (A) Combined training progression for all data layers, illustrating convergence and network stability. (B) Training dynamics for individual data layers, highlighting their relative contributions to map formation. (C) Feature importance, showing the influence of each morphological, ecological, and genetic variable on cluster assignment. (D) Estimation of the optimal number of clusters based on network stability and convergence metrics.